Quantitative electron holography of magnetic fields in nanoscale materials and devices

M.R. McCartney[1], T. Kasama[2] and R.E. Dunin-Borkowski[2]

1. Department of Physics, Arizona State University, Tempe, AZ 85287-1504, U.S.A.
2. Center for Electron Nanoscopy, Technical University of Denmark, 2800 Lyngby, Denmark

molly.mccartney@asu.edu
Keywords: electron holography, phase shift, magnetic induction

Off-axis electron holography is a powerful technique that can be used to characterize magnetic and electrostatic fields in materials in the transmission electron microscope (TEM) with sub-10-nm spatial resolution [1, 2]. In its standard form, electron holography involves applying a positive voltage to an electron biprism in order to overlap a coherent electron wave that has passed through a specimen with a part of the same electron wave that has passed through vacuum. Analysis of the resulting interference pattern allows the phase shift of the specimen wave to be recovered quantitatively and non-invasively. For medium resolution applications, the objective lens is turned off and a mini-lens is used for imaging, allowing for a larger field of view and the possibility of magnetic-field-free imaging. Here, we present several recent applications of the technique to the measurement of magnetic fields and discuss its possible future development.

The off-axis electron holograms that are presented below were acquired at accelerating voltages of either 200 or 300 kV using field emission gun TEMs equipped with a 'Lorentz' lens and an electron biprism located close to the conventional selected area aperture plane of the microscope. The holograms were recorded digitally, either with the conventional microscope objective lens switched off and the specimen located in magnetic-field-free conditions, or with the objective lens used to provide an applied field. Reference holograms were used to remove distortions associated with the imaging and recording system of the microscope.

Nanoscale ring-shaped magnetic elements are of interest for magnetic recording and storage applications because they can support flux-closed (FC) magnetic states that would not be stable in disk-shaped elements of similar size. Figure 1 shows magnetic contributions to the phase shift and induction maps from three self-assembled rings of 25-nm-diameter polycrystalline Co nanoparticles recorded using off-axis electron holography. Each particle comprises a core of hexagonal-close-packed crystals of Co and a shell of ~3 nm of CoO [3]. Holograms were recorded in zero-field conditions after applying chosen out-of-plane (OOP) magnetic fields *in situ* in the TEM by partially exciting the conventional microscope objective lens. The mean inner potential (MIP) contribution to the phase shift was calculated from phase images that had been acquired before and after turning the specimen over. Their sum and difference were used to determine twice the MIP and twice the magnetic contribution to the phase shift, respectively. Once the MIP contribution had been determined, it could be subtracted from all subsequent phase images acquired from the same region of the specimen. The resulting phase images were smoothed slightly, and phase contours and colors were used to form the final induction maps. An OOP field of -20,000 Oe was initially applied perpendicular to the plane of the specimen and reduced to zero. The sample was then taken out of the TEM in zero field, turned over and put back into the microscope. Chosen OOP fields of up to +20,000 Oe were then applied to the specimen in the TEM in succession by changing the current in the TEM objective lens. The applied field was reduced to zero before recording each hologram. Although the initial chiralities (directions of magnetization) of the

W. Grogger, F. Hofer, P. Pölt (Eds.): MC2009, Vol. 3: Materials Science,
DOI: 10.3217/978-3-85125-062-6-381 , © Verlag der TU Graz 2009

FC states in the individual rings are determined by the shapes, sizes and positions of the constituent nanoparticles, reproducible magnetization reversal of most rings could be achieved by using OOP fields of between 1600 and 2500 Oe. The switching behavior was compared with micromagnetic simulations, which suggested that metastable states form at intermediate applied fields prior to FC reformation at remanence.

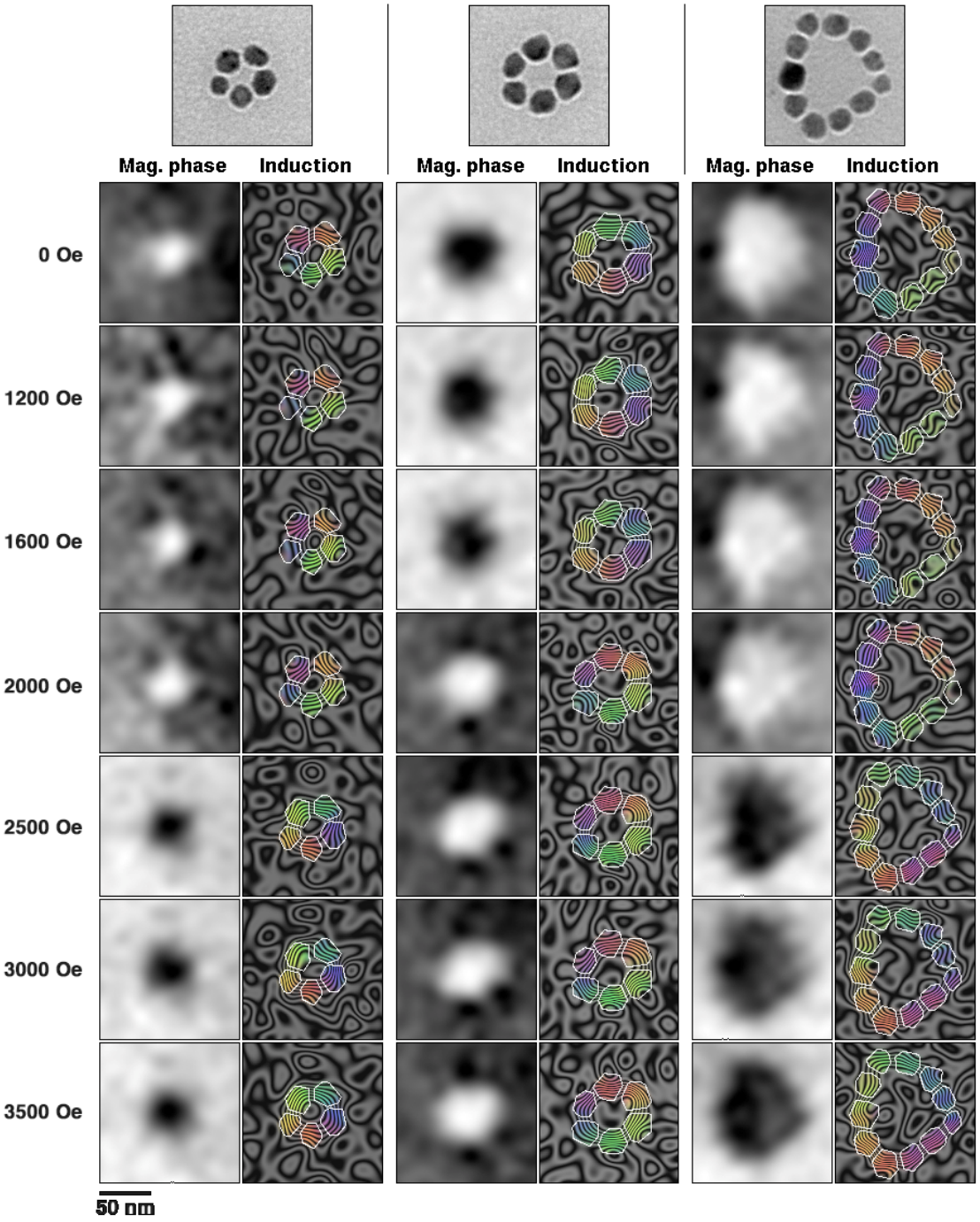

Figure 1. *Top row*: Defocused bright-field TEM images of rings of polycrystalline Co nanoparticles. *Subsequent rows*: Magnetic contributions to the phase shift and induction maps recorded at remanence using off-axis electron holography after initially saturating the rings using a large (-20,000 Oe) out-of-plane magnetic field and then applying the indicated out-of-plane fields in succession. The direction of the projected induction is shown using both contours and colors (red=right; blue=up; green=left; yellow=down). The contour spacing is 0.065 rad, corresponding to 96 × phase amplification.

W. Grogger, F. Hofer, P. Pölt (Eds.): MC2009, Vol. 3: Materials Science,
DOI: 10.3217/978-3-85125-062-6-381 , © Verlag der TU Graz 2009

Attention has recently been directed towards studies of multilayered spin-valve structures because of their practical giant magnetoresistance properties for magnetic sensors and recording devices, as well to provide a fundamental understanding of the strong interactions that are likely to be present between the two adjacent ferromagnetic layers. Results obtained from a slotted-ring spin-valve element consisting of 12 nm of Co, 6 nm of Cu and 12 nm of permalloy (Py), patterned directly onto a 50-nm-thick silicon nitride membrane using electron beam lithography, are shown in Fig. 2. A 2-nm-thick Ti layer was deposited after lift-off to avoid oxidation and to prevent electrostatic charging during TEM observation. A hysteresis loop was recorded by applying an out-of-plane field using partial excitation of the objective lens, while the sample was tilted between +30° and -30°. The gradients of the phase shifts within the elements, calculated perpendicular to the applied field direction, were normalized to the saturation values (recorded at the highest tilt angles) to provide a measure of the magnetization, which is plotted as a function of applied field in Fig. 2. It is notable that the softer Py layer reverses before the applied field reaches zero due to coupling with the fringing field of the Co layer [4].

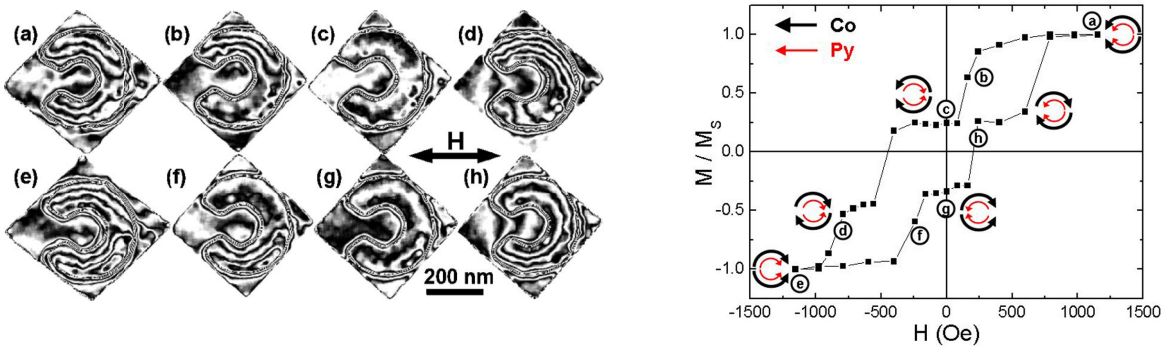

Figure 2. Reconstructed contoured phase images of a Co/Cu/Py spin-valve element, illustrating the magnetization configurations of corresponding states in the hysteresis loop. The applied fields are parallel to the slot direction, horizontally from right to left for (a)-(d) and from left to right for (e)-(h). The three-step hysteresis loop, which was measured from the same spin-valve element, shows the different magnetic configurations of the Co and Py layers during the hysteresis cycle.

Figure 3 illustrates a similar application of electron holography to nanoscale magnetic device structures that were patterned directly onto a Si substrate, and so were challenging to prepare for electron microscopy without damaging the magnetic properties of the regions of interest on the specimen. The magnetic layers in this specimen are also narrower and thinner than those in Fig. 2. Figure 3a shows a scanning electron micrograph of the sample, which comprises nominally identical 75×280 nm pseudo-spin-valve elements prepared from polycrystalline $Ni_{79}Fe_{21}$ (4.1 nm)/ Cu (3 nm)/ Co (3.5 nm)/ Cu (4 nm) sputtered onto oxidized Si. An approach based on focused ion-beam milling with Ga ions, which is described in Fig. 3b, was used to minimize damage to the magnetic properties of the elements during preparation for TEM examination in plan-view geometry. Figure 4 shows six magnetic induction maps of three adjacent elements recorded at remanence after saturating the elements magnetically either parallel or antiparallel to their length using the field of the microscope objective lens, followed by applying a reverse field [5]. These images were used to identify separate switching of the Co and NiFe layers in the individual elements and to measure their switching fields, as shown in the form of a remanent hysteresis loop in Fig. 5. A comparison of Fig. 5 with micromagnetic simulations suggests that ~20 nm of material at the edge of each element does not contribute to the magnetic signal, possibly as a result of

DOI: 10.3217/978-3-85125-062-6-381 , © Verlag der TU Graz 2009

oxidation during fabrication. In addition, the in-plane component of the induction in the Co layer is reduced by ~ 40% from its nominal value. Differences in hysteresis between the elements are observed, and are thought to result from microstructural variations. Such variability must be minimized if similar elements are to be used in ultra-high density recording applications.

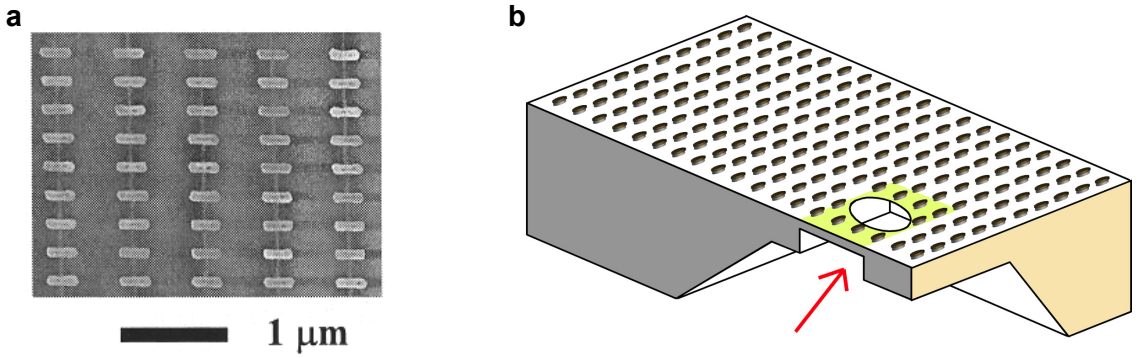

Figure 3. (a) Scanning electron micrograph showing a rectangular array of 75 nm x 280 nm NiFe/Cu/Co pseudo-spin-valve elements. (b) Schematic diagram illustrating the final stage of the procedure used to prepare an electron-transparent plan-view sample of the pseudo-spin-valve elements for electron holography, by using focused ion-beam milling with Ga ions. A piece of the wafer is initially milled from the substrate side at one corner. A membrane is formed parallel to the wafer surface. A hole is then formed in this membrane by milling from below, at a glancing angle to the original wafer surface. In this way, the elements that are on the near side of the hole are protected from ion damage and implantation by the intervening substrate, and the hole can subsequently be used to provide a reference wave for electron holography.

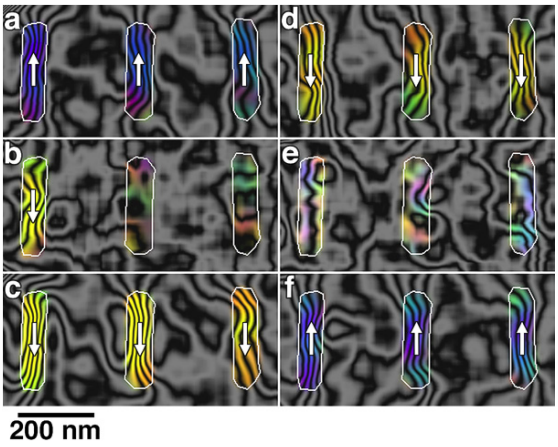

Figure 4. Magnetic induction maps showing six remanent magnetic states recorded using electron holography from three pseudo-spin-valve elements. 18 images similar to these were recorded in total. The outlines of the elements are shown in white. The contour spacing is $2\pi/64=0.098$ rad, such that the magnetic flux enclosed between any two adjacent black contours is $h/64e=6.25\text{x}10^{-17}$ Wb. The direction of the induction is shown using arrows and colors (red=right, yellow=down, green=left, and blue=up).

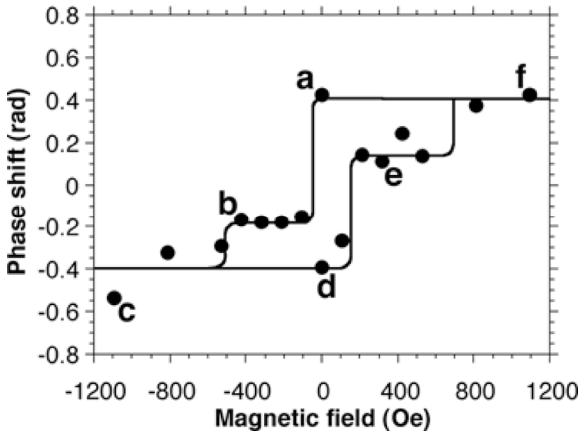

Figure 5. Remanent hysteresis loop measured directly from the experimental electron holographic phase images, with the letters corresponding to the six individual figures shown in Fig. 4. The graph shows the magnetic contribution to the phase shift across each element, plotted as a function of the in-plane component of the field applied to the elements before recording the remanent states. Each point shows an average of the phase shifts measured from the three elements shown in Fig. 4.

W. Grogger, F. Hofer, P. Pölt (Eds.): MC2009, Vol. 3: Materials Science,
DOI: 10.3217/978-3-85125-062-6-381 , © Verlag der TU Graz 2009

Figures 6 and 7 illustrate the application of electron holography to the study of naturally occuring ferrimagnetic magnetite (Fe_3O_4) crystals that are arranged either in linear chains inside magnetotactic bacteria [6] or in the form of finely-exsolved arrays of magnetic minerals in rocks [7]. The magnetic induction maps highlight the fact that the sizes, shapes and arrangements of the crystals are optimized for use as internal magnetic compasses in the bacteria (Fig. 6) and as stable recorders of the ancient geomagnetic field in rocks (Fig. 7).

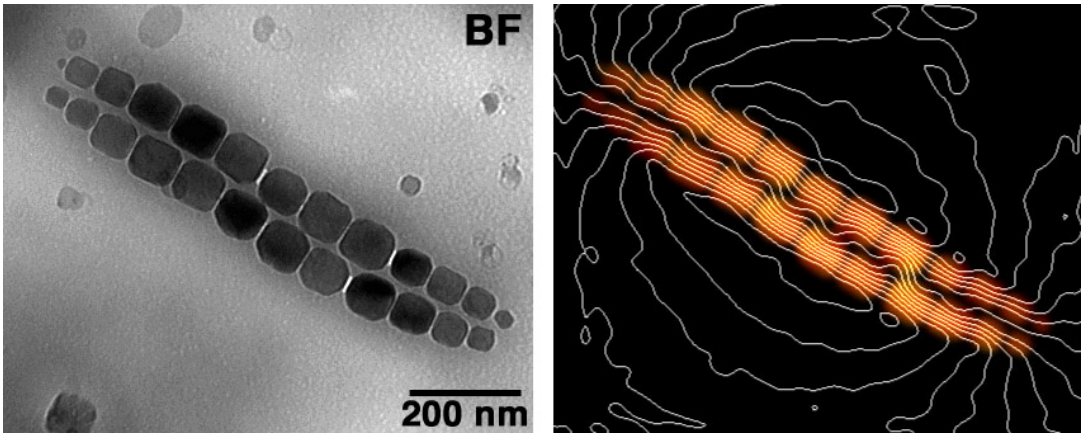

Figure 6. Bright-field (BF) image (left) and magnetic induction map (right) of a double chain of magnetite nanocrystals from a magnetotactic bacterial cell. Interactions between neighboring magnetite nanocrystals decrease the critical size at which the transition from superparamagnetic to single domain behavior occurs.

Figure 7. (a) Chemical map of naturally occurring titanomagnetite, obtained using a Gatan imaging filter. Blue regions show magnetite (Fe_3O_4) blocks, which are separated from each other by paramagnetic ulvöspinel (Fe_2TiO_4). (b) and (c) show magnetic phase contours measured using electron holography from the same region, acquired after magnetizing the sample in different directions using the magnetic field of the microscope objective lens. The colors show the directions of the magnetic induction.

Figure 8 illustrates the use of Lorentz TEM, electron holography and a TEM specimen holder that allows multiple electrical contacts to be made to an electron-transparent specimen to study the competing effects of heating and spin torque on the current-induced motion of transverse and vortex-type domain walls in permalloy wires [8].

W. Grogger, F. Hofer, P. Pölt (Eds.): MC2009, Vol. 3: Materials Science,
DOI: 10.3217/978-3-85125-062-6-381 , © Verlag der TU Graz 2009

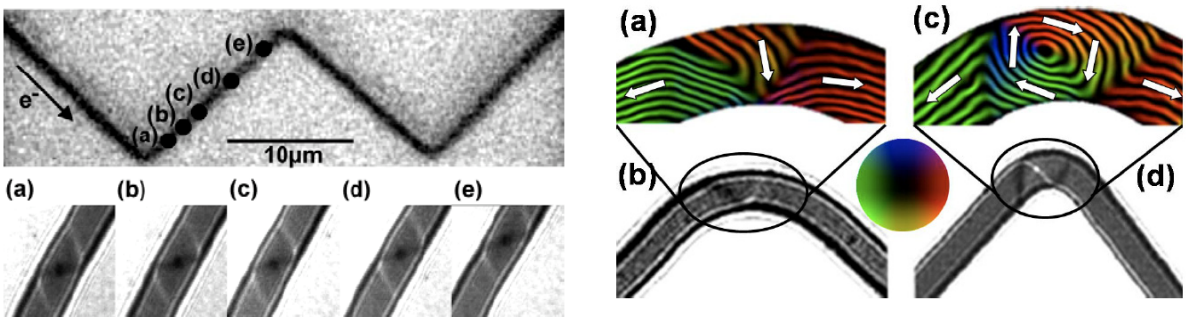

Figure 8. Use of electrical biasing specimen holder to study domain wall motion and transformations following the injection of current pulses along zigzag permalloy structures patterned lithographically on silicon nitride windows. The images were acquired using both the Fresnel mode of Lorentz electron microscopy and electron holography (top right).

The work that is described above has resulted from the development of new approaches for the acquisition, analysis and simulation of electron holograms, the design and use of specimen holders that allow electrical contacts to be applied to magnetic devices *in situ* in the electron microscope, and the comparison of recorded magnetic induction maps both with micromagnetic simulations and with three-dimensional information about the local compositions and morphologies of the same specimens acquired using electron tomography. In particular, it has required the development of new approaches for the careful separation of the weak magnetic signal of primary interest from unwanted contributions to recorded holographic phase contrast. The resulting ability to study magnetic states and switching phenomena with nanometer spatial resolution can be used to initiate new research fields. The work is also important for the development of a fundamental experimental understanding of magnetic domain structures, reversal mechanims, coercivities and interactions in isolated and closely-spaced magnetic nanoparticles and deep-submicron device structures, including the identification of the shapes and arrangements of magnetic elements that are stable, reversible and reproducible at room temperature for future applications in magnetic recording and storage. Further work is required to optimize specimen preparation for medium resolution electron holography, to increase the sensitivity of the technique for measuring weak fields, to improve its time resolution, and to understand the effect of specimen preparation and electron irradiation on measurements of both magnetic and electrostatic fields. The prospect of characterizing magnetic vector fields *inside* nanocrystals in three dimensions by combining electron tomography with electron holography is also of great interest [9, 10].

1. M.R. McCartney and D.J. Smith, Ann. Rev. Mater. Res. **37** (2007) 729
2. J.M. Thomas et al., Acc. Chem. Res. **41** (2008) 665
3. T. Kasama et al., Adv. Mat. **20** (2008) 4248
4. K. He et al., Appl. Phys. Lett. **94** (2009) 172503
5. T. Kasama et al., J. Appl. Phys. **98** (2005) 013903
6. R.E. Dunin-Borkowski et al., Science **282** (1998) 1868.
7. J.M. Feinberg et al., J. Geophys. Res. **111** (2006) B12S15
8. F. Junginger et al., Appl. Phys. Lett. **90** (2007) 132506
9. T. Kasama et al., Mater. Res. Soc. Proc. **839** (2005), Pittsburgh, PA, P5.01
10. We thank RIKEN, the Royal Society, the EPSRC and the US Department of Energy (DE-FG02-04ER46168) for support. We are also grateful to E.A. Fischione Instruments for specimen holder development and to A. Wei, C.A. Ross, M. Pósfai, R.J. Harrison, J.M. Feinberg, M. Kläui and S.B. Newcomb for ongoing collaborations.